Engineering phonon-photon interactions with a driven trapped ion in a cavity

R. L. Rodrigues, M. H. Y. Moussa, and C. J. Villas-Bôas
Departamento de Física, Universidade Federal de São Carlos, P.O. Box 676, São Carlos, 13565-905, São Paulo, Brazil
(Received 12 July 2006; published 12 December 2006)

We show how to generate quadratic and biquadratic phonon-photon interactions through a driven three-level ion inside a cavity. With such a system it is possible to squeeze the cavity-field state, the ion motional state, or even the entangled phonon-photon state. We present a detailed analysis of the cavity-field squeezing process, distinguishing three different regimes of this amplification mechanism: the subcritical, critical, and supercritical regimes, which depend, apart from the coupling parameters, on the excitation of the vibrational state. As an application of the engineered Hamiltonians, we show how to implement a Fock-state filter for the vibrational mode. Different aspects of the technique of adiabatic elimination emerge in this analysis.

DOI: 10.1103/PhysRevA.74.063811 PACS number(s): 42.50.Dv, 32.80.−t, 42.50.Ct

I. INTRODUCTION

Together with cavity quantum electrodynamics (QED) and manipulation of light states through linear and nonlinear optical elements, the physics of trapped ions is a major ingredient of the quantum information theory research scene. The experimental achievements aligned with the theoretical propositions in these domains of quantum optics have contributed significantly to the insertion of quantum information theory in virtually all the areas of nowadays physics. The possibility to insert a trapped ion inside a cavity to manipulate phonon-photon interaction has been raised from the very beginning of the period of experimental accomplishments in cavity QED and trapped ions [1]. Since then, the problem of phonon-photon interaction with a trapped ion inside a cavity has attracted attention, owing to its application to quantum logic operation [2–4], to the translation of phonon to photon statistics or the transference of squeezing from phonons to photons [5], and to the study of the dynamics of the interaction between a cavity field and the motional degrees of freedom of a trapped ion [6]. A scheme for quantum swapping between vibrational and cavity field states has also been presented [7], not to mention that the engineering of quantum states in such a system, specially of entangled atomic motion and cavity field [8], is considered in all these references. Parallel to the study and applications of phonon-photon interaction, the major mechanisms of decoherence in ionic traps have been experimentally analyzed [9] and modeled [10–12]. The knowledge acquired over the last few years about dissipative mechanisms in both systems, high-Q cavities, and ionic traps, has resulted in protocols for quantum-state protection in ionic traps [13] and cavity QED [14].

In the present paper we are interested in engineering phonon-photon interactions with a trapped ion inside a cavity. The program of engineering Hamiltonians has become a major concern in quantum information research: beyond the need for quantum state preparation, a given logical operation requires specific interactions between the subsystems comprising the quantum bits. Recent work has been devoted to engineering bilinear interactions in two-mode cavity QED; specifically, parametric up- and down-conversion operations were accomplished through the dispersive interactions of the cavity modes with a single three-level-driven atom which works as a nonlinear medium [15–18]. Here, a three-level trapped ion interacting simultaneously with a classical field and a single cavity mode will be treated by the adiabatic approximation technique. Different aspects of this approximation are revealed through our analysis which handles both the weak and the strong-amplification regimes of the classical field.

II. THE MODEL

The energy diagram of the three-level trapped ion, sketched in Fig. 1, is in the ladder configuration, where the ground $|g\rangle$ and excited $|e\rangle$ states, with transition frequency ω_0, are coupled through an intermediate level $|i\rangle$. The cavity mode of frequency ω is tuned to the vicinity of both dipole-allowed transitions, $|g\rangle \leftrightarrow |i\rangle$ and $|e\rangle \leftrightarrow |i\rangle$, with coupling constants λ_1 and λ_2 and detunings $\delta_1=\Delta+\delta$ and $\delta_2=\Delta-\delta$, respectively, where $\delta=\omega_0/2-\omega$. Simultaneously to the cavity mode, a classical field is assumed to drive resonantly the dipole-forbidden atomic transition $|g\rangle \leftrightarrow |e\rangle$ with coupling constant Ω [19]. The Hamiltonian which describes this system is given by $H=H_0+V(t)$, where (with $\hbar=1$)

$$H_0 = \omega a^\dagger a + \nu b^\dagger b + (\omega+\delta)(\sigma_{ee}-\sigma_{gg}) + \Delta\sigma_{ii}, \tag{1a}$$

$$V(t) = (\lambda_1\sigma_{gi} + \lambda_2\sigma_{ie})(a^\dagger + a)\sin(\eta(b^\dagger + b) + \varphi) + \Omega\exp[-2i(\omega+\delta)t]\sigma_{eg}\exp[i\eta_L(b^\dagger + b)] + \text{H.c.}, \tag{1b}$$

with $a^\dagger$ (a) and $b^\dagger$ (b) standing for the creation (annihilation) operators of the quantized cavity mode and the one-dimensional trapped motion of frequency ν, while $\sigma_{rs} \equiv |r\rangle\langle s|$ (r,s being the atomic states g,e,i). The Lamb-Dicke parameter $\eta_L=k_L/\sqrt{2m\nu}$ ($\eta=k/\sqrt{2m\nu}$) follows from the interaction of the ion with the classical (quantum) radiation field characterized by the wave vector $k_L=\omega_L/c$ ($k=\omega/c$). Finally, φ accounts for the relative position of the ion in the cavity standing wave, such that $\varphi=0$ ($\pi/2$) corresponds to an ion centered at a node (antinode) of the standing wave. The phase accounting for the relative position of the ion with respect to the classical field is incorporated into the complex constant $\Omega=|\Omega|e^{-i\phi}$. After the unitary transformations U_0

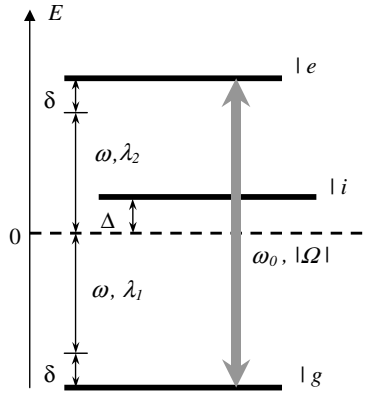

FIG. 1. Energy diagram of the three-level trapped ion in the ladder configuration.

$=\exp(-iH_0t)$ and $U_1=\exp(i\Delta\sigma_{ii}t)$, associated with the interaction picture and a frame rotating with frequency Δ, respectively, the Hamiltonian becomes $\mathcal{H}=U_1^\dagger U_0^\dagger H U_0 U_1 - H_0 + \Delta\sigma_{ii}$. Assuming from here on that $\omega \gg \nu, \delta, \Delta, \lambda_1, \lambda_2$ and keeping terms of order of η^2 within the Lamb-Dicke limit $\eta^3 \ll 1$, we obtain within the rotating-wave approximation (neglecting terms rotating with frequency of the order of 2ω):

$$\mathcal{H}(t) = [(\lambda_1\sigma_{gi} + \lambda_2\sigma_{ie})a^\dagger \Lambda(b,b^\dagger;t) + \Omega\sigma_{eg}\Sigma(b,b^\dagger;t) + \text{H.c.}] + \Delta\sigma_{ii}, \tag{2}$$

where the time-dependent functions for the trapped-motion operators are given by

$$\Lambda(b,b^\dagger;t) = \exp(-i\delta t)\exp(-i\nu b^\dagger b t)\sin(\eta(b^\dagger + b) + \varphi_c)\exp(i\nu b^\dagger b t), \tag{3a}$$

$$\Sigma(b,b^\dagger;t) = \exp(-i\nu b^\dagger b t)\exp[i\eta_L(b^\dagger + b)]\exp(i\nu b^\dagger b t). \tag{3b}$$

Defining a new basis for the atomic states $\{|i\rangle, |\pm\rangle = [|e\rangle \pm e^{i\phi}|g\rangle]/\sqrt{2}\}$ [20], composed of eigenstates of the atomic Hamiltonian $|\Omega|(e^{-i\phi}\sigma_{eg} + e^{i\phi}\sigma_{eg})$, and assuming the Lamb-Dicke-like limit $\eta_L \ll 1$, such that $\Sigma(b,b^\dagger;t) \approx 1$, we obtain

$$\mathcal{H}(t) = \frac{1}{\sqrt{2}}[(\lambda_1 e^{-i\phi}a^\dagger\Lambda + \lambda_2^* a\Lambda^\dagger)\sigma_{+i} - (\lambda_1 e^{-i\phi}a^\dagger\Lambda - \lambda_2^* a\Lambda^\dagger)\sigma_{-i} + \text{H.c.}] + \Delta\sigma_{ii} + |\Omega|(\sigma_{++} - \sigma_{--}). \tag{4}$$

The adiabatic approximation

Next, we proceed with a two-step approach for the adiabatic elimination of both transitions $|+\rangle \leftrightarrow |i\rangle$ and $|-\rangle \leftrightarrow |i\rangle$. In the first step we write, from the Liouville-von Neumann equation $\dot{\rho} = -i[\mathcal{H}(t), \rho]$, the operator $\dot{\rho}_{rs}$ associated with the transition $|r\rangle \leftrightarrow |s\rangle$ (with $r,s = +,-,i$). Imposing the condition $\dot{\rho}_{+i} = \dot{\rho}_{-i} = 0$, we obtain the adiabatic solutions for both operators ρ_{+i} and ρ_{-i}. The substitution of these solutions back into $\dot{\rho}_{++}$, $\dot{\rho}_{--}$, and $\dot{\rho}_{ii}$ results in the evolution operators for the probabilities of measuring the electronic states $|+\rangle$, $|-\rangle$, and $|i\rangle$, respectively. Next, in the second step, assuming that the Hamiltonian under the adiabatic approximation (superscript A) is given by

$$\mathcal{H}(t) = \mathcal{H}^A_{++}\sigma_{++} + \mathcal{H}^A_{--}\sigma_{--} + \mathcal{H}^A_{ii}\sigma_{ii} + (\mathcal{H}^A_{+-}\sigma_{+-} + \text{H.c.}), \tag{5}$$

in which the unwanted transitions are missing, we employ again the Liouville-von Neumann equation to write new transition operators $\dot{\rho}^A_{rs}$. Comparing the operators $\dot{\rho}^A_{++}$, $\dot{\rho}^A_{--}$, and $\dot{\rho}^A_{ii}$, with those obtained previously in the first step, $\dot{\rho}_{++}$, $\dot{\rho}_{-}$, and $\dot{\rho}_{ii}$, we finally obtain the Hamiltonian terms $\mathcal{H}^A_{++}$, $\mathcal{H}^A_{--}$, $\mathcal{H}^A_{ii}$, $\mathcal{H}^A_{+-}$, and $\mathcal{H}^A_{-+}$. The validity of the adiabatic approximation follows from that of the adiabatic solutions

$$|\Delta \pm |\Omega|| \gg |\lambda_1|, |\lambda_2|, \delta, \tag{6}$$

which leads to two different regimes of parameters: (i) the weak-amplification regime, where $\Delta \gg |\Omega|, |\lambda_1|, |\lambda_2|, \delta$, and (ii) the strong-amplification regime, where $|\Omega| \gg \Delta, |\lambda_1|, |\lambda_2|, \delta$. We note that the technique of adiabatic elimination, as used in the literature to date, applies only to the weak-amplification regime. The strong-amplification regime defined above is another complementary aspect of adiabatic elimination. The resulting Hamiltonian terms are given by

$$\mathcal{H}^A_{\ell k} = \{\omega_{\ell k}a^\dagger a + \chi_{\ell k} + [\xi_{\ell k}e^{-i2\delta t}(a^\dagger)^2 + \text{H.c.}]\}VV^\dagger, \tag{7}$$

with $\ell, k = +,-,i$, $V = U_0^\dagger \sin[\eta(b^\dagger + b)]\ U_0$; defining, in the weak (w) and strong (s)-amplification regimes, effective frequencies (ω_w, ω_s), coupling strengths (ξ_w, ξ_s), and energy shifts (χ_w, χ_s), as

$$\omega_w = \frac{|\lambda_1|^2 + |\lambda_2|^2}{\Delta}, \quad \omega_s = \frac{|\lambda_1|^2 + |\lambda_2|^2}{|\Omega|},$$

$$\xi_w = \frac{\lambda_1\lambda_2 e^{-i\phi}}{\Delta}, \xi_s = \frac{\lambda_1\lambda_2 e^{-i\phi}}{|\Omega|},$$

$$\chi_w = \frac{|\lambda_1|^2}{\Delta}, \quad \chi_s = \frac{|\lambda_1|^2}{|\Omega|}, \tag{8}$$

the Hamiltonian parameters read, in the weak-amplification regime:

$$\omega_{ii} \sim \omega_w, \quad \chi_{ii} \sim \chi_w, \quad \xi_{ii} \sim -\frac{|\Omega|}{\Delta}\xi_w,$$

$$\omega_{++} \sim -\frac{1}{2}\omega_w, \quad \chi_{++} \sim -\frac{|\lambda_2|^2}{2|\lambda_1|^2}\chi_w, \quad \xi_{++} \sim -\frac{1}{2}\xi_w,$$

$$\omega_{--} \sim \omega_{++}, \quad \chi_{--} \sim \chi_{++}, \quad \xi_{--} \sim -\xi_{++},$$

$$\omega_{+-} \sim \frac{|\lambda_1|^2 - |\lambda_2|^2}{2\Delta}, \quad \chi_{+-} \sim \chi_{++}, \quad \xi_{+-} \sim \xi_{++}, \tag{9}$$

and in the strong-amplification regime:

$$\omega_{ii} \sim -\frac{\Delta}{|\Omega|}\omega_s, \quad \chi_{ii} \sim -\frac{\Delta}{|\Omega|}\chi_s, \quad \xi_{ii} \sim -\xi_s,$$

$$\omega_{++} \sim -\frac{1}{2}\omega_s, \quad \chi_{++} \sim \frac{|\lambda_2|^2}{2|\lambda_1|^2}\chi_s, \quad \xi_{++} \sim \frac{1}{2}\xi_w,$$

$$\omega_{--} \sim -\omega_{++}, \quad \chi_{--} \sim -\chi_{++}, \quad \xi_{--} \sim \xi_{++},$$

$$\omega_{+-} \sim 0, \quad \chi_{+-} \sim 0, \quad \xi_{+-} \sim 0. \tag{10}$$

Note that in the weak-amplification regime, the states $|+\rangle$ and $|-\rangle$ couple to each other through dynamical evolution, while in the strong-amplification regime each state evolves independently. This fact represents an additional advantage of the strong coupling regime, apart from the considerably stronger couplings that require shorter atom-field interaction times for manipulations of the cavity or the vibrational mode, making the dissipative mechanisms almost negligible.

III. THE ENGINEERED INTERACTIONS

Preparing the ion in the state $|i\rangle$, we obtain from the Hamiltonian in Eq. (7), returning to the Schrödinger picture, the result

$$H = \omega a^\dagger a + \nu b^\dagger b + \{\omega_{ii} a^\dagger a + \chi_{ii} + [\xi_{ii} e^{-2i(\omega+\delta)t}(a^\dagger)^2 + \text{H.c.}]\}\sin^2[\eta(b^\dagger + b) + \varphi], \tag{11}$$

which will be analyzed in two cases corresponding to the ion centered at a node or an antinode of the standing wave, $\varphi = 0$ or $\pi/2$, respectively:

$$\sin^2(\eta(b^\dagger + b) + \varphi) \approx \begin{cases} 1, & \text{adjusting } \eta^2 \ll 1 \text{ and } \varphi = \pi/2, \\ \eta^2(b^\dagger + b)^2, & \text{adjusting } \eta^4 \ll 1 \text{ and } \varphi = 0. \end{cases} \tag{12}$$

Analyzing the case where $\sin^2(\eta(b^\dagger+b)+\varphi) \approx 1$, in the interaction picture defined by the transformation $U = \exp\{-i[(\omega+\omega_{ii})a^\dagger a + \nu b^\dagger b]t\}$, we obtain, in both weak and strong-amplification regimes, the first engineered Hamiltonian

$$\mathbf{H}_1 = \xi_{ii}(a^\dagger)^2 + \text{H.c.}, \tag{13}$$

where we have adjusted the cavity mode such that $\delta = \omega_{ii}$. Interestingly enough, this Hamiltonian leads to the squeezing operator acting only on the cavity mode: $S(\xi_{ii}, t) = \exp[-i(\xi_{ii} a^{\dagger 2} + \xi_{ii}^* a^2)t]$.

Given that $\xi_{ii} = |\xi_{ii}| e^{i\Theta}$, the degree of squeezing of the cavity field state achieved through Hamiltonian $\mathbf{H}_1$ [Eq. (13)] is determined by the factor $r(t) = 2|\xi_{ii}|t$, while the squeeze angle is given by $\Theta/2$. For a specific cavity mode and electronic configuration of the trapped ion (i.e., for specific λ_1, λ_2, and Δ), the parameter $r(t)$ can be adjusted in accordance with the coupling strength $|\Omega|$ and the interaction time t. To estimate the degree of squeezing achieved we assume trapped Rydberg atoms. Thus considering typical cavity QED values for the parameters involved, arising from Rydberg levels where the intermediate state $|i\rangle$ is nearly halfway between $|g\rangle$ and $|e\rangle$, with $\Delta \sim 3 \times 10^6\ \text{s}^{-1}$, we get $|\lambda_1| \sim |\lambda_2| \sim 3 \times 10^5\ \text{s}^{-1}$ [21]. In the weak-amplification regime, such values lead to $\delta = \omega_{ii} = \omega_w \sim 6 \times 10^4\ \text{s}^{-1}$, and assuming the coupling strength $\Omega \sim 3 \times 10^5\ \text{s}^{-1}$, we obtain $|\xi_{ii}| \sim 3 \times 10^3\ \text{s}^{-1}$. Therefore for an ion-field interaction time about $t \sim 2 \times 10^{-4}$ s, we get the squeezing factor $r(t) \sim 1.2$ such that the squeezing rate turns out to be $\mathcal{R} = (1 - e^{-2r(t)}) \times 100\% \sim 91\%$ (for an initial coherent state prepared in the cavity). A laser pulse of longer duration leads to a squeezing rate even greater than this remarkable rate (at the expense of intensifying the dissipative mechanisms, neglected in the present work). Note that the interaction time adopted here is one order of magnitude smaller than the decay time of the open cavities used in cavity QED experiments [21]. Evidently, for the strong-amplification regime, we will obtain an even higher degree of squeezing for the cavity mode.

We note that our cascade atomic-level scheme, where an auxiliary intermediate state $|i\rangle$ is used to couple the dippole-forbidden transition $|g\rangle \leftrightarrow |e\rangle$, differs from the schemes used by both trapped ion groups: at NIST [22], concentrated on Lambda configuration, and Innsbruck [23], where a dipole forbidden transition $|g\rangle \leftrightarrow |e\rangle$ is induced by applying a sufficiently strong electric field. However, the values presented above for the atomic frequencies and couplings, arising from the Rydberg levels used in Ref. [21], are around those considered in the Innsbruck configuration.

Next, to handle the case $\sin^2(\eta(b^\dagger+b)+\varphi) \approx \eta^2(b^\dagger+b)^2$, it is convenient to consider a picture defined by the transformation $U = \exp\{-i[\omega a^\dagger a + \Phi b^\dagger b]t\}$, where the Hamiltonian reads

$$\mathbf{H} = \eta^2(2b^\dagger b + 1)\{\omega_{ii} a^\dagger a + [\xi_{ii} e^{-2i\delta t}(a^\dagger)^2 + \text{H.c.}]\} + \eta^2(\omega_{ii} a^\dagger a + \chi_{ii})[e^{2i\Phi t}(b^\dagger)^2 + \text{H.c}] + \eta^2[\xi_{ii} e^{-2i(\delta-\Phi)t}(a^\dagger)^2(b^\dagger)^2 + \text{H.c.}] + \eta^2[\xi_{ii} e^{-2i(\delta+\Phi)t}(a^\dagger)^2(b)^2 + \text{H.c.}], \tag{14}$$

and $\Phi = \nu + 2\eta^2\chi_{ii}$. Evidently, varying the choice of the detuning δ leads to distinct interactions, such that, by adjusting δ to Φ and $-\Phi$, we obtain in both amplification regimes, after rotating wave approximations, respectively,

$$\mathbf{H}_2 = \eta^2\omega_{ii}(2b^\dagger b + 1)a^\dagger a + \eta^2[\xi_{ii}(a^\dagger)^2(b^\dagger)^2 + \text{H.c.}], \tag{15a}$$

$$\mathbf{H}_3 = \eta^2\omega_{ii}(2b^\dagger b + 1)a^\dagger a + \eta^2[\xi_{ii}(a^\dagger)^2(b)^2 + \text{H.c.}], \tag{15b}$$

where we have assumed, whatever the state of the cavity mode, the condition $\Phi \gg \omega_{ii}\langle a^\dagger a\rangle + \chi_{ii}$, ξ_{ii}. Under this same condition, but with $|\delta| \ll \Phi$, also in both amplification regimes, we obtain the time-dependent interaction

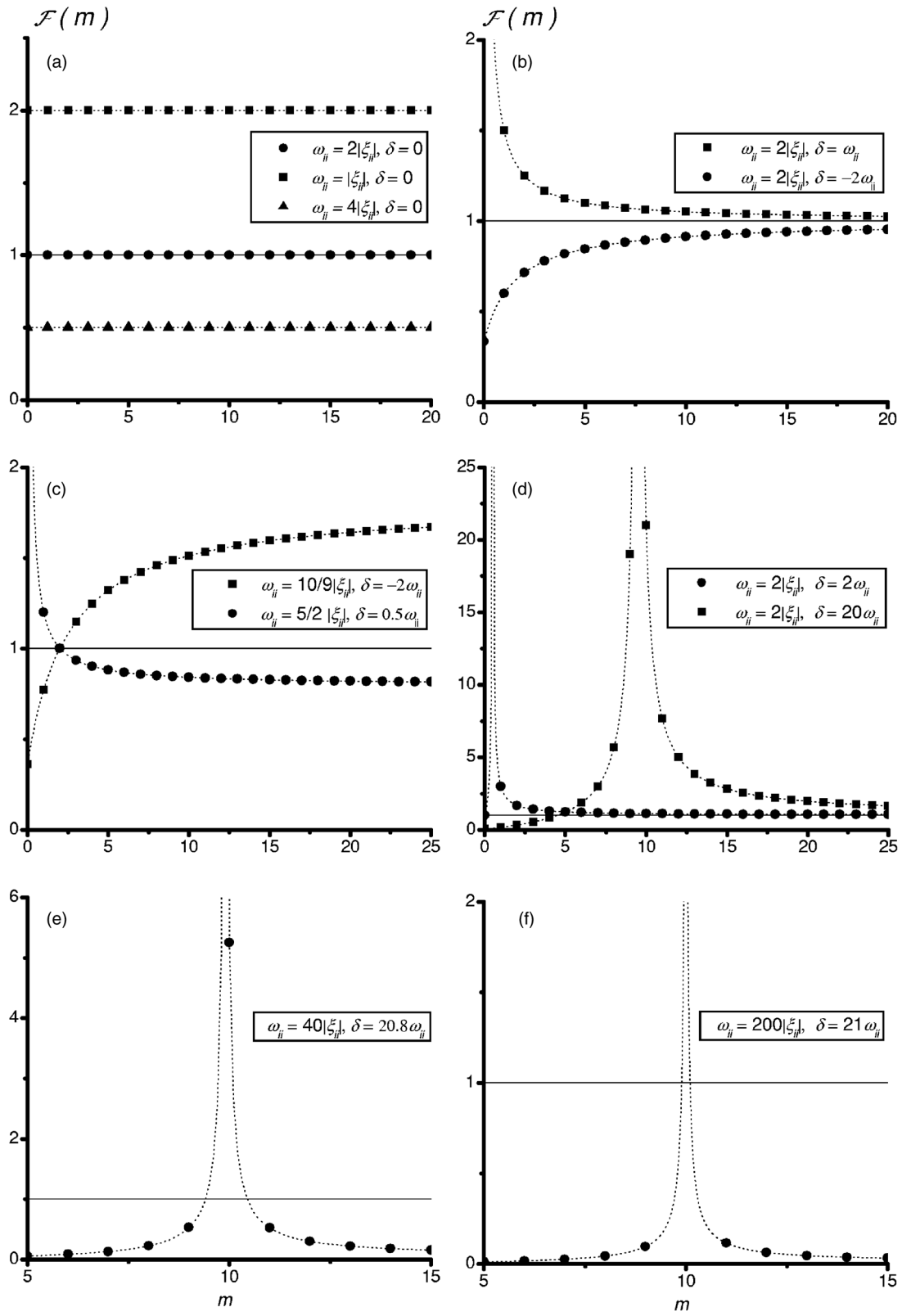

FIG. 2. Distinct forms of behavior of $\mathcal{F}(m)$, for different values of ω_{ii} and δ, which determines the regimes of the parametric amplification processes.

$$\mathbf{H}_4 = \eta^2(2b^\dagger b + 1)\{\omega_{ii}a^\dagger a + [\xi_{ii}e^{-2i\delta t}(a^\dagger)^2 + \text{H.c.}]\}. \quad (16)$$

Finally, with $|\delta| \sim |\Phi|$ and $|\delta \pm \Phi| \sim |\Phi|$, or $\delta \sim 0$ and $\xi_{ii} \ll \omega_{ii}$, we obtain the Kerr-like interaction

$$\mathbf{H}_5 = \eta^2\omega_{ii}a^\dagger a(2b^\dagger b + 1), \quad (17)$$

which is suitable for introducing phases into one field state, according to the intensity of the other.

IV. THE HAMILTONIAN $\mathbf{H}_4$

A. Subcritical, critical, and supercritical regimes

To understand the behavior of the system under the approximations leading to Hamiltonian $\mathbf{H}_5$, its would be helpful to eliminate the time-dependence of the interaction $\mathbf{H}_4$ through the unitary transformation $U_{SC}(t)=\exp[-i\delta t a^\dagger a]$. We are left with the simplified form

$$\mathbf{H}_4 = \Xi(b^\dagger b)a^\dagger a + \frac{1}{2}[\Gamma(b^\dagger b)(a^\dagger)^2 + \text{H.c.}], \tag{18}$$

where the functions for the trapped-motion operators are given by

$$\Xi(b^\dagger b) = \eta^2\omega_{ii}(2b^\dagger b + 1) - \delta, \tag{19a}$$

$$\Gamma(b^\dagger b) = 2\eta^2\xi_{ii}(2b^\dagger b + 1). \tag{19b}$$

In the Fock basis representation for the vibrational operators, the $b^\dagger b$ operator is replaced by the motional excitation m and the Hamiltonian (18) becomes

$$\mathbf{H}_4(m) = \Xi(m)\left[a^\dagger a + \frac{1}{2}[\mathcal{F}(m)(a^\dagger)^2 + \text{H.c.}]\right], \tag{20}$$

where the function $\mathcal{F}(m)$ stands for the ratio

$$\mathcal{F}(m) = \frac{\Gamma(m)}{\Xi(m)} = \frac{2\xi_{ii}/\omega_{ii}}{1 - \delta/[2\omega_{ii}(m + 1/2)]}. \tag{21}$$

Evidently, for $\Xi(m)=0$, we obtain the resonant amplification regime leading to the maximum degree of squeezing of the cavity field. For $\Xi(m)\neq 0$, the absolute value $|\mathcal{F}(m)|$ determines three different regimes of the nonresonant parametric amplification process, the subcritical ($|\mathcal{F}|<1$), critical ($|\mathcal{F}|=1$), and supercritical ($|\mathcal{F}|>1$) regimes. These regimes are characterized by oscillatory, linear, and hyperbolic solutions of the Heisenberg equations of motion for the evolution of the annihilation operator of the cavity mode given by

$$a(t) = f(t)a - ig(t)a^\dagger, \tag{22}$$

where the time-dependent functions in the subcritical, critical, and supercritical regimes are

$$f_{<1}(t) = \cos[\varpi(m)t] - i\frac{\Xi(m)}{\varpi(m)}\sin[\varpi(m)t], \tag{23a}$$

$$f_{=1}(t) = 1 - i\varpi(m)t, \tag{23b}$$

$$f_{>1}(t) = \cosh[\varpi(m)t] - i\frac{\Xi(m)}{\varpi(m)}\sinh[\varpi(m)t], \tag{23c}$$

and

$$g_{<1}(t) = \frac{\Gamma(m)}{\varpi(m)}\sin[\varpi(m)t], \tag{24a}$$

$$g_{=1}(t) = \Gamma(m)t, \tag{24b}$$

$$g_{>1}(t) = \frac{\Gamma(m)}{\varpi(m)}\sinh[\varpi(m)t], \tag{24c}$$

where $\varpi^2(m)=||\Gamma(m)|^2-\Xi^2(m)|$. Evidently, for $|\mathcal{F}|\gg 1$, we are close to the resonant regime. Each of these regimes results in a different squeezing process of the cavity-field state, as already discussed in Refs. [14,24]. However, since in the present model the vibrational field is an additional ingredient, for fixed values of δ, η, ω_{ii}, and ξ_{ii}, the various regimes can be achieved by manipulating the excitation number m of the vibrational mode, except in some particular cases where the adjustment of the detuning δ results in a fixed amplification regime for all values of m. These are the cases of Fig. 2(a), where $\delta=0$ leads to the constant function $\mathcal{F}=2\xi_{ii}/\omega_{ii}$, and Fig. 2(b), where δ is adjusted in such a way that $|\mathcal{F}|<1$ or $|\mathcal{F}|>1$ for all m. In Fig. 2(c), the parameters are adjusted to get an inversion of the behavior of function $\mathcal{F}$, from $|\mathcal{F}|\leqslant 1$ to $|\mathcal{F}|\geqslant 1$, passing or not through $|\mathcal{F}|=1$. We note that in Figs. 2(b) and 2(c) the decreasing functions are singular for $m=0$ where we have the resonant amplification regime. In Figs. 2(a)–2(c) $|\mathcal{F}|$ behaves nonmonotonically. With the parameters of Fig. 2(d), we obtain two different behaviors with the same ω_{ii}: for $\delta=20\omega_{ii}$, we start from the subcritical regime (passing or not through the critical regime with a suitable adjustment of δ), while for $\delta=2\omega_{ii}$ we begin from the critical regime at $m=0$. In both cases, the critical regime is reached assymptotically from the supercritical regime. In Fig. 2(e) we have the subcritical regime for all values of m except for $m=10$, at which the supercritical regime is found. Finally, in Fig. 2(f) we have the same behavior as in Fig. 2(e), except that for $m=10$ we have a singularity, indicating the resonant regime for this value of m.

In the case where the vibrational field is prepared in a coherent state β, it is possible to choose the mean excitation $|\beta|^2$ in such a way that all the significant values for its Fock components m lie in the subcritical or supercritical region. As an example, within the parameters of Fig. 2(c) and a coherent state $\beta\sim 4$, we obtain the supercritical (subcritical) regime for all the significant values of m when $\omega_{ii}=(10/9)|\xi_{ii}|$ and $\delta=-2\omega_{ii}$ [$\omega_{ii}=(10/4)|\xi_{ii}|$ and $\delta=0.5\omega_{ii}$].

B. A Fock state filter

Let us consider $\delta=\omega_{ii}(2M+1)$, where the resonant regime occurs only for $m=M$ and the subcritical regime at all other values of m, as in Fig. 2(f). Starting from the cavity mode in the vacuum state and the vibrational mode in a coherent state $|\beta\rangle=\Sigma_m C_m|m\rangle$, we obtain from Hamiltonian $\mathbf{H}_4(m)$ the evolved superposition

$$|\psi(t)\rangle = C_M|M\rangle S_M(t)|0\rangle + \sum_{\substack{m=0 \\ (m\neq M)}}^{\infty} C_m|m\rangle S_m(t)|0\rangle, \tag{25}$$

where $S_M(t)=\exp[-i[\Gamma(M)(a^\dagger)^2+\text{H.c.}]t/2\}$ stands for the ideal squeezing operator and $S_m(t)=\exp[-i\mathbf{H}_4(m)t]$ indicates the nonresonant squeezing operator in the subcritical regime. Adjusting $\omega_{ii}\gg|\xi_{ii}|$, such that $\varpi(m)\sim|\Xi(m)|$ and $|\Gamma(m)/\Xi(m)|\sim|\xi_{ii}|/\omega_{ii}\ll 1$, the squeezing process is strongly

nonresonant for all values of m other than M. Consequently, there will be practically no photon injection into the cavity mode from the nonresonant squeezing (NS) process, since

$$\langle a^\dagger a\rangle_{NS} = (1-|C_M|^2)^{-1} \sum_{\substack{m=0 \\ (m\neq M)}}^{\infty} |C_m|^2 \langle 0|S_m^\dagger(t) a^\dagger a S_m(t)|0\rangle$$

$$= (1-|C_M|^2)^{-1} \sum_{\substack{m=0 \\ (m\neq M)}}^{\infty} |C_m|^2 \left|\frac{\Gamma(m)}{\varpi(m)}\right|^2 \sin^2(|\varpi(m)|t)$$

$$\leqslant \frac{|\xi_{ii}|}{\omega_{ii}}. \tag{26}$$

Therefore, for such a nonresonant process, the cavity field remains close to the vacuum state. On the other hand, the resonant squeezing (RS) process accounts for a significant photon injection into the cavity mode, whose excitation becomes

$$\langle a^\dagger a\rangle_{RS} = \langle 0|S_M^\dagger(t) a^\dagger a S_M(t)|0\rangle = \sinh^2[|\Gamma(M)|^2 t]. \tag{27}$$

Therefore, after a convenient time interval t, when $\langle a^\dagger a\rangle_{RS}$ is appreciably larger than unity, a measurement of the cavity field, in a state with a considerable number of photons, will project the vibration mode into the Fock state $|M\rangle$. Evidently, the probability of success in generating the number state $|M\rangle$, given by $|C_M|^2 = e^{-|\beta|^2}|\beta|^{2M}/M!$, can be maximized by adjusting the amplitude of the coherent state β. This measurement is accomplished by passing through the cavity a stream of ground-state two-level atoms interacting resonantly with the cavity mode [25].

C. The semiclassical approximation

Next, we analyze Hamiltonian (16) for the supercritical case and the semiclassical approximation where the annihilation (creation) operator b ($b^\dagger$) is replaced by the amplitude β (β^*) of a strong coherent state. [Note that this procedure must be carried out from the initial model in Eq. (2), so that the factor $(2b^\dagger b+1)$ in Eq. (16) should be replaced by $|\beta|^2$.] Adjusting the detuning between the cavity field and the atom such that $\delta = 2\eta^2|\beta|^2\omega_{ii}$, the unitary transformation $U_{SC}(t) = \exp[-i\delta t a^\dagger a]$ allows us to rewrite Hamiltonian $\mathbf{H}_5$ in its semiclassical form

$$\mathbf{H}_{SC} = 2\eta^2|\beta|^2[\xi_{ii}(a^\dagger)^2 + \text{H.c.}],$$

which describes an ideal squeezing process with the squeezing factor given by $r = 4\eta^2|\beta|^2|\xi_{ii}|t$. Therefore, the larger the amplitude β, the shorter the time required to attain a given degree of squeezing. To estimate the validity of this approximation we compare the variance of the squeezed quadrature $(\Delta X_{sq})^2$ computed from the two Hamiltonians, Eqs. (16)—under the same transformation U_{SC}—and (18). In Fig. 3 we plot $(\Delta X_{sq})^2$ against the squeezing factor r, where $X_{sq} \equiv (a + a^\dagger)/2$, for different values of the coherent vibrational state β, assumed to be real. Since the abscissa represents the squeezing factor r, the straight line in Fig. 3 describes the evolution of variance $(\Delta X_{sq})^2$ governed by the semiclassical Hamiltonian $\mathbf{H}_{SC}$, for any value $\beta > 0$. On the other hand, the dotted, dashed-dotted, and dashed lines describe $(\Delta X_{sq})^2$ for the full quantum Hamiltonian $\mathbf{H}_5$, taking $\beta = 1$, 5, and 10, respectively. As expected, the larger the value of the amplitude of the vibrational field β, the better the semiclassical approximation. For $\beta = 10$, the variance obtained through the semiclassical interaction fits the quantum description to a good approximation for a degree of squeezing about 90%, i.e., $r \sim 1$, which is achieved in a time interval about $4 \times 10^2 \times \eta^2|\xi_{ii}|^{-1}$ s.

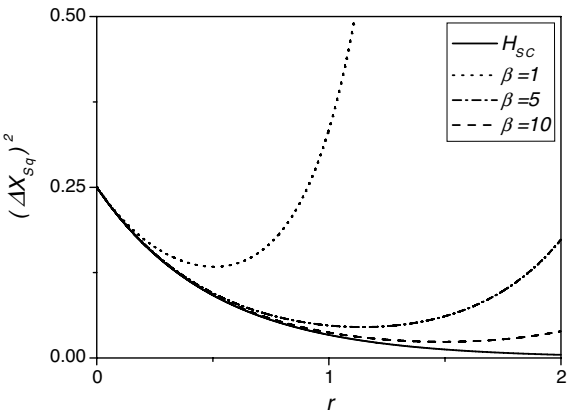

FIG. 3. The variance of the squeezed quadrature $(\Delta X_{sq})^2$ against the squeezing factor r for the semiclassical Hamiltonian $\mathbf{H}_{SC}$ and for the full quantum Hamiltonian $\mathbf{H}_5$, for $\beta = 1$, 5, and 10.

V. CONCLUSIONS

In this paper we have presented a scheme for engineering quadratic and biquadratic phonon-photon interactions through a driven three-level ion inside a cavity. The adiabatic approximation was employed and different aspects of this technique were revealed through our analysis. Umtil now, this approximation has been applied only in the weak-amplification regime, where the atom-field coupling parameters are considerably smaller than their detunings. In our approach, we also considered the strong-amplification regime where, in contrast, the detunings were made considerably smaller than the atom-field coupling parameters.

A detailed analysis of the squeezing process of the cavity mode was accomplished by considering a particular phonon-photon interaction, described by Hamiltonian (16), revealing the possibility of one resonant and three different nonresonant regimes of parametric amplification of the cavity mode. Interestingly enough, such regimes of parametric amplification can be modulated through the excitation of the vibrational-field state. We also showed how to generate, through the same Hamiltonian (16), a filter of any Fock state for the vibrational mode via a projective measurement of the cavity-field state.

Finally, we presented a detailed analysis of the semiclassical approximation which enabled us to replace the opera-

tors describing the vibrational field in Hamiltonian (16) by classical amplitudes, simplifying considerably this interaction. The same analysis of the validity of the semiclassical regime can be carried out for Hamiltonians (15). It is worth mentioning a recent achievement by Guthöhrlein *et al.* [26], where a near-field probe with atomic-scale resolution, a single calcium ion in a radio-frequency trap, is reported. This work opens the way for performing higher resolution cavity quantum electrodynamics experiments with a single trapped particle.

ACKNOWLEDGMENTS

We wish to express thanks for the support from PIADRD/UFSCar, FAPESP, CAPES, and CNPq (Instituto do Milênio de Informação Quântica), Brazilian agencies. We also thank R. M. Serra for helpful discussions.

[1] F. E. Harrison, A. S. Parkins, M. J. Collett, and D. F. Walls, Phys. Rev. A **55**, 4412 (1997).
[2] X. B. Zou, K. Pahlke, and W. Mathis, Phys. Rev. A **65**, 064303 (2002).
[3] F. L. Semiao, A. Vidiella-Barranco, and J. A. Roversi, Phys. Lett. A **299**, 423 (2002); F. L. Semiao and A. Vidiella-Barranco, Phys. Rev. A **72**, 064305 (2005).
[4] M. Feng and X. G. Wang, J. Opt. B: Quantum Semiclassical Opt. **4**, 283 (2002).
[5] M. Orszag, Laser Phys. **12**, 1054 (2002).
[6] C. Di Fidio and W. Vogel, J. Opt. B: Quantum Semiclassical Opt. **4**, 342 (2002).
[7] R. Rangel, E. Massoni, and N. Zagury, Phys. Rev. A **69**, 023805 (2004).
[8] C. Di Fidio, S. Maniscalco, W. Vogel, and A. Messina, Phys. Rev. A **65**, 033825 (2002).
[9] D. M. Meekhof, C. Monroe, B. E. King, W. M. Itano, and D. J. Wineland, Phys. Rev. Lett. **76**, 1796 (1996).
[10] C. Di Fidio and W. Vogel, Phys. Rev. A **62**, 031802(R) (2000).
[11] R. M. Serra, N. G. de Almeida, W. B. da Costa, and M. H. Y. Moussa, Phys. Rev. A **64**, 033419 (2001).
[12] A. A. Budini, R. L. de Matos Filho, and N. Zagury, Phys. Rev. A **65**, 041402(R) (2002).
[13] A. R. R. Carvalho, P. Milman, R. L. de Matos Filho, and L. Davidovich, Phys. Rev. Lett. **86**, 4988 (2001).
[14] C. J. Villas-Bôas, N. G. de Almeida, and M. H. Y. Moussa, Phys. Rev. A **60**, 2759 (1999); J. Opt. B: Quantum Semiclassical Opt. **5**, 391 (2003).
[15] C. J. Villas-Böas, N. G. de Almeida, R. M. Serra, and M. H. Y. Moussa, Phys. Rev. A **68**, 061801(R) (2003).
[16] R. M. Serra, C. J. Villas-Boas, N. G. de Almeida, and M. H. Y. Moussa, Phys. Rev. A **71**, 045802 (2005).
[17] C. J. Villas-Boas and M. H. Y. Moussa, Eur. Phys. J. D **32**, 147 (2005).
[18] R. Guzmán, J. C. Retamal, E. Solano, and N. Zagury, Phys. Rev. Lett. **96**, 010502 (2006).
[19] This dipole-forbidden transition can be induced by taking advantage of dipole-allowed transitions to another auxiliary level. In this case, a fourth level $|f\rangle$ must be added to the atomic system together with appropriate classical fields inducing a Raman transition with effective couplings given by $\Omega = g_1^* g_2/\tilde{\Delta}$, g_1 and g_2 being the coupling constants in the vicinity of the dipole-allowed transitions $|g\rangle \leftrightarrow |f\rangle$ and $|e\rangle \leftrightarrow |f\rangle$, both with detuning $\tilde{\Delta} \gg |g_1|, |g_2|$. For the strong-coupling regime, it is required that $\Omega \sim 10^6\ \mathrm{s}^{-1}$, which follows from $g_1 \sim g_2 \sim 10^7\ \mathrm{s}^{-1}$ (easily achieved for dipole-allowed transitions). Note that we may also consider the auxiliary level $|i\rangle$ itself for this purpose, taking care to keep the classical fields far from resonance with the cavity modes.
[20] E. Solano, G. S. Agarwal, and H. Walther, Phys. Rev. Lett. **90**, 027903 (2003); see also S. B. Zheng, Phys. Rev. A **66**, 060303(R) (2002).
[21] J. M. Raimond *et al.*, Rev. Mod. Phys. **73**, 565 (2001).
[22] D. J. Wineland, C. Monroe, W. M. Itano, D. Leibfried, B. E. King, and D. M. Meekhof, J. Res. Natl. Inst. Stand. Technol. **103**, 259 (1998).
[23] D. Leibfried, R. Blatt, C. Monroe, and D. Wineland, Rev. Mod. Phys. **75**, 281 (2003).
[24] B. Baseia, S. S. Mizrahi, and M. H. Y. Moussa, Phys. Rev. A **46**, 5885 (1992); S. S. Mizrahi, M. H. Y. Moussa, and B. Baseia, Int. J. Mod. Phys. B **8**, 1563 (1994).
[25] M. Brune, S. Haroche, J. M. Raimond, L. Davidovich, and N. Zagury, Phys. Rev. A **45**, 5193 (1992).
[26] G. R. Guthöhrlein, M. Keller, K. Hayasaka, W. Lange, and H. Walther, Nature (London) **414**, 49 (2001).